

Experimental study on thermoelectric modules for power generation at various operating conditions

Wei-Hsin Chen^{a,*}, Chen-Yeh Liao^b, Chen-I Hung^b, Wei-Lun Huang^c

^a Department of Greenergy, National University of Tainan, Tainan 700, Taiwan, ROC

^b Department of Mechanical Engineering, National Cheng Kung University, Tainan 701, Taiwan, ROC

^c Genesis Combustion Technology Incorporation, Tainan 711, Taiwan, ROC

ARTICLE INFO

Article history:

Received 21 January 2012

Received in revised form

29 June 2012

Accepted 29 June 2012

Available online 31 July 2012

Keywords:

Thermoelectric module and generator

Power generation

Waste-heat recovery

Series connection

Peltier effect

ABSTRACT

Commercially available thermoelectric modules are useful devices to recover low-temperature waste heat for power generation. To understand the characteristics of power generation from thermoelectric modules (TEMs), the performances of TEMs at various flow patterns, heating temperatures, flow rates of water and numbers of modules in series are studied experimentally. The results show that the effects of flow pattern of heat sink and water flow rate on the performance are not significant, but the heat source or heating temperature plays an important role. Therefore, a lower water flow rate is suggested to save power, whereas a higher hot-side temperature which leads to a larger temperature difference is recommended to give better performances of TEMs. Increasing number of modules in series provide higher output power. However, the performance of the modules in series cannot be simply predicted using linear superposition due to the Peltier effect and the non-uniformity of every module. The feature of a thermoelectric generator (TEG) is also examined and compared with the TEMs. It is found that TEM is a better choice for power generation from recovering waste heat if the temperature of a system is below 150 °C.

© 2012 Elsevier Ltd. All rights reserved.

1. Introduction

Thermoelectric (TE) devices can be used for power generation and refrigeration. TE devices designed to generate power through the Seebeck effect are called TE generators (TEGs). TE coolers/modules (TECs/TEMs) are the devices which are operated for cooling purpose via the Peltier effect [1,2]. Compared to the conventional generators or coolers, TE devices have numerous advantages such as no moving parts to cause vibration or noise, high reliability and environmental friendly [3,4]. Therefore, over the last decade much attention has been paid to the related research. For example, for TECs or TEMs, the influence of scaling effect and Thomson effect on their performances has been investigated [5,6]. Some studies developed the concept of thermoelectric self-cooling [7] and the combination of TECs and solar cells for green building [8]. Meanwhile, the effect of irreversibilities [9] on the performance of TEGs and the feasibility of heat from stoves for TEGs have been discussed [10,11].

As far as TEG is concerned, its conversion is a simple and reliable solid-state technology [12]. In addition, its conversion is the most

effective among several processes, say, thermoelectric, thermomagnetism, ferroelectricity and the Nernst effect, which can transform thermal energy into electricity [1,13]. One should note that the efficiency of thermoelectric conversion is still low, typically around 5% [14]. Other proposing technology such as organic Rankine cycle (ORC), which converts the low- and medium-temperature heat to electricity, can yield efficiencies of 9–11% [15,16]. Hence, TEGs have restricted its use to specialized medical, military and space applications, such as radioisotope power for deep space probes, and remote power, such as oil pipelines and sea buoys, where cost is not a main consideration. Because of this, much effort has been made to improve the intrinsic conversion efficiency of TE materials [17,18]. However, the low efficiency is no longer the major issue when waste heat is recovered as a heat source because of its low-cost and even no-cost [14,19]. In some studies [20,21], the system efficiency can even be improved through using waste heat.

Seeing that TEGs can be employed for power generation by recovering waste heat as a heat source, much research has been done. For example, some attention has been paid to the recovery of waste heat from automobiles. Thacher et al. [12] tested the performance of 16 HZ-20 generators which were connected in series and placed in automobile exhaust. They found that output

* Corresponding author. Tel.: +886 6 2605031; fax: +886 6 2602205.

E-mail address: weihsinchen@gmail.com (W.-H. Chen).

Nomenclature

I	Electric current (A)
M	Number of variables (dimensionless)
N	Number of thermoelectric modules in series (dimensionless)
n	Number of measured data (dimensionless)
P	Power (W)
S_f	Uncertainty
S_x	Sample standard deviation
T	Temperature ($^{\circ}\text{C}$)
V	Voltage (V)
X	Measured data
\bar{X}	Mean value of measured data

Greek letters

Δ	Temperature difference ($^{\circ}\text{C}$)
----------	---

Subscript

c	Cold side
H	Heating surface
h	Hot side
l	Load
oc	Open circuit
out	Output
max	Maximum
w	Water

power was limited by the heat exchanger of hot side and the maximum allowed operating temperature. Hsiao et al. [22] built a one-dimensional thermal resistance model to predict the behavior of TE system applied in exhaust pipe and radiator of an automobile. They reported that the temperature difference across the TEG and the output power increased as the engine speed or the coolant temperature increased, and the performance of the TEG placed on the exhaust pipe was better than on the radiator. Anatyshuk et al. [23] investigated the behavior of TEGs applied on the exhaust pipe of an automobile and reported that the temperature distribution along the TEGs was exponential. They concluded that the half of the TEGs operated under high temperature conditions so that using low-temperature TEGs was not appropriate in the tested system. Min and Rowe [24] developed a procedure to assess the potential of thermoelectric modules (TEMs) used for power generation. They noted that TEMs originally designed for cooling purpose were promising devices for power generation through recovering waste heat in the temperature range of 300–400 K in that TEMs possess the merit of lower cost compared to TEGs. Hence TEMs can be chosen in the TE system for the low-temperature waste heat recovery.

The low-temperature heat source usually causes low performance of TE system. Some researchers thus focused on the influences of heat exchanger, heat source and heat transfer capability on the TE system. Esarte et al. [25] used an NTU- ϵ methodology to discuss the effects of heat exchanger geometry, fluid flow rate, fluid properties and inlet temperature on the output power of the TEG system. Yu and Zhao [26] presented a numerical model of the TEG with parallel-plate heat exchanger. They observed that the larger inlet temperature and flow rate of the hot fluid led to the higher output power and efficiency; but the increasing trend became smaller when the flow rate kept increasing. Niu et al. [27] further connected 56 TEMs in series with parallel-plate heat exchanger and low-temperature waste heat to validate their previous numerical model [26]. Astrain et al. [28] developed a computational model

and their results suggested that the improvement on thermal resistances at both sides of heat exchangers was important. Gou et al. [29] established a theoretical model and constructed a low-temperature waste heat recovery system with 10 TEMs in series. They found that increasing waste heat temperature and adding TEMs in series could enhance the performance of the setup. Hsu et al. [30] simulated and tested the performance of a waste heat recovery system which comprised 24 TEGs in series. Zhu et al. [31] studied the influence of heat source power, hot-side temperature, load resistance and Peltier effect on the performance of TEG by a series of experiments. They also discussed the performance of TEGs in parallel. It was reported that a loop current was produced from the non-uniformity among parallel TEGs so that the loading capability of the overall power system was decreased. Liang et al. [32] further proposed the analytical model of parallel TEG and they found that the parallel characteristics of two parallel TEGs were different from common DC power due to the non-uniformity between the TEGs.

Despite the parallel connection of TEGs conducted [31,32], the serial connection was absent. In the study of Gou et al. [29], the effect of TEMs in series on power generation has been analyzed theoretically; but experiments were absent. For these reasons, the present study is intended to experimentally explore the performances of TEMs under various combinations. Unlike fluids or heat exchangers were utilized in certain studies, the present study adopts heaters to provide thermal energy into the hot side of the modules. Other parameters such as the heating temperature and the flow pattern and flow rate of cold fluid will also be discussed.

2. Experimental method

2.1. Experimental apparatus and procedure

A schematic of the experimental system is shown in Fig. 1. The system was made up of a heater, aluminum plates, TEMs, heat sinks, a cold fluid loop, four compressive loads, an electronic load and a data acquisition unit. The heater was used to continuously supply

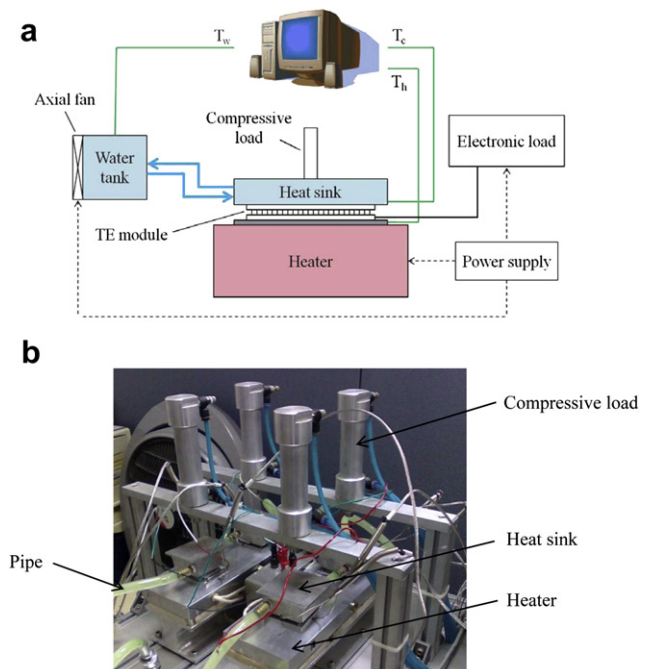


Fig. 1. (a) Schematic of investigation system and (b) picture of experimental setup.

thermal energy to the hot side of the TEMs. The aluminum plates were placed between the heater and the modules to make temperature measurement of the hot sides more convenient. The TEMs were used as generators through thermoelectric conversion. The heat sinks were attached to the cold sides of the modules to remove the residual thermal energy by the cold fluid loop. The cold fluid loop included a tank (5 L), an axial fan, a pump, a flow meter (Honsberg Rototron RRI-010/050), pipes and a coolant. The coolant was water because it is available, harmless to the environment. Besides, in the studies of Meng et al. [9] and Feeley et al. [33], it was pointed out that water represented a growing concern for meeting future power generation needs. The residual thermal energy was delivered to the tank by water and then to the surrounding by the axial fan. The water flow rate was controlled by adjusting the input voltage of the pump. The interfaces between the modules, aluminum plates and heat sinks were covered thermal grease to reduce the thermal contact resistance. The compressive loads attached to the heat sinks were also used to diminish the gaps and thermal contact resistances of the interfaces. The electronic load (Chroma 6312A & 63102A) was used to simulate the external load and to measure the output voltage and power of the modules. The temperatures of hot side, cold side and water were measured by thermocouples which were placed at appropriate locations. All the data were collected and recorded by the data acquisition system.

2.2. Performance evaluation

The temperature difference between the hot and cold sides is obtained as the following

$$\Delta T = T_h - T_c \quad (1)$$

where T_h and T_c are the temperatures of the hot and the cold sides, respectively. The output power (W) is calculated by

$$P_{\text{out}} = IV_l \quad (2)$$

where I is the electrical current (A) and V_l is the output voltage (V). They both are measured from the electronic load.

2.3. Experimental quality

Before experiments were carried out, the electronic load and flow meter as well as thermocouples were calibrated to ascertain their accuracies. The operating or measuring value and the resolutions of the equipments are tabulated in Table 1. The relative

uncertainties of the adopted equipments are listed in the table as well. The relative uncertainty of the equipment is defined as [34]

$$\text{Relative uncertainty} = \frac{0.5 \times \text{resolution}}{\text{operating or measuring value}} \quad (3)$$

It can be seen that the relative uncertainty due to the equipments is no larger than 2.5%. To provide an error analysis of experiments, Table 1 also lists the data of temperatures, voltage and current in the experiments where the heating temperature (T_h) and water flow rate were controlled at 150 °C and 1.0 L min⁻¹, respectively. In a set of data, the mean value (\bar{X}) and standard deviation (S_X) of the data are defined by [35]

$$\bar{X} = \frac{1}{n} \sum_{i=1}^n X_i \quad (4)$$

$$S_X = \left[\frac{1}{n-1} \sum_{i=1}^n (X_i - \bar{X})^2 \right]^{1/2} \quad (5)$$

As can be seen in Table 1, the uncertainty (=Mean value/Standard deviation × 100) is controlled around or below 5.7%. In addition, the multiplication of V_l and I will have the maximum output power. Therefore, the uncertainty of the maximum power is estimated at 2.14% as follows [35]

$$S_J = \left[\sum_{i=1}^M (S_J)_i^2 \right]^{1/2} \quad (6)$$

$$\frac{\delta P_{\text{max}}}{P_{\text{max}}} = \left[\left(\frac{\delta V_l}{V_l} \right)^2 + \left(\frac{\delta I}{I} \right)^2 \right]^{1/2} = \left[(2.1)^2 + (0.4)^2 \right]^{1/2} = 2.14\% \quad (7)$$

Because the uncertainty of measurement is below 6%, this reveals that the experiments in the current study are reliable.

3. Results and discussion

Four TEMs labeled from Nos. 1 to 4 and a TEG were considered for investigation. The physical sizes and characteristics of the TEMs and TEG are listed in Table 2. The main parameters regarded for study included the flow pattern of coolant (i.e. water) in heat sink, heating temperatures, flow rates of water and numbers of modules in series. Two different flow patterns in heat sinks were taken in

Table 1
A list of equipment uncertainty and experiment uncertainty.

Equipment uncertainty						
Equipment	Operating or measuring range			Resolution	Relative uncertainty	
Heater	110–150 °C			0.1 °C	0.1%	
Flowmeter	0.4–1.6 L min ^{−1}			0.01 L min ^{−1}	1.3%	
Electronic load (for voltage)	0.46–19.54 V			0.00125 V	0.1%	
Electronic load (for electric current)	0.10–1.40 A			0.005 A	2.5%	
Experiment uncertainty						
Variable	Measure value @60 min			Mean value	Sample standard deviation	Uncertainty
	1st	2nd	3rd			
T_h	134.5 °C	138.9 °C	137.7 °C	137.0 °C	2.3 °C	1.7%
T_c	37.4 °C	41.9 °C	40.0 °C	39.8 °C	2.3 °C	5.7%
T_w	29.8 °C	28.0 °C	30.8 °C	29.5 °C	1.4 °C	4.8%
V_{oc}	4.9725 V	4.8725 V	4.9225 V	4.9225 V	0.0500 V	1.0%
V_l (@ P_{max})	2.5275 V	2.4225 V	2.4725 V	2.4742 V	0.0525 V	2.1%
I (@ P_{max})	0.705 A	0.700 A	0.705 A	0.703 A	0.002 A	0.4%

Table 2
Physical sizes and characteristics of thermoelectric modules and generator.

Thermoelectric module (in cooling mode)	
Type number	TECCP-24-001
No. of TE couples	127
Length \times width \times height (mm ³)	40 \times 40 \times 3.3
I_{\max} , allowed (A)	10
U_{\max} , allowed (V)	8.5
Q_{\max} , allowed (W)	94.2
ΔT_{\max} , allowed (°C)	66
Thermoelectric generator	
Type number	TG-12-8-01L
Length \times width \times height (mm ³)	44 \times 40 \times 3.6
$T_{H, \max}$, allowed (°C)	250

account. The heating temperature of the heater was between 110 and 150 °C since the maximum allowed operating temperature of the TEMs was 150 °C. The flow rate of water was between 0.4 and 1.6 L min⁻¹. When the TEMs in series were explored, they were connected thermally in parallel and electrically in series from 1 to 4. The compressive loads were set at 60 psi. In each run, the experimental duration was 2 h. The main output parameters were the temperature difference between the hot and cold sides, output voltage and power of the modules.

3.1. Effect of flow pattern and temporal temperature distribution

First of all, No. 1 module in association with two kinds of heat sink named Types A and B was tested in the study. The difference of

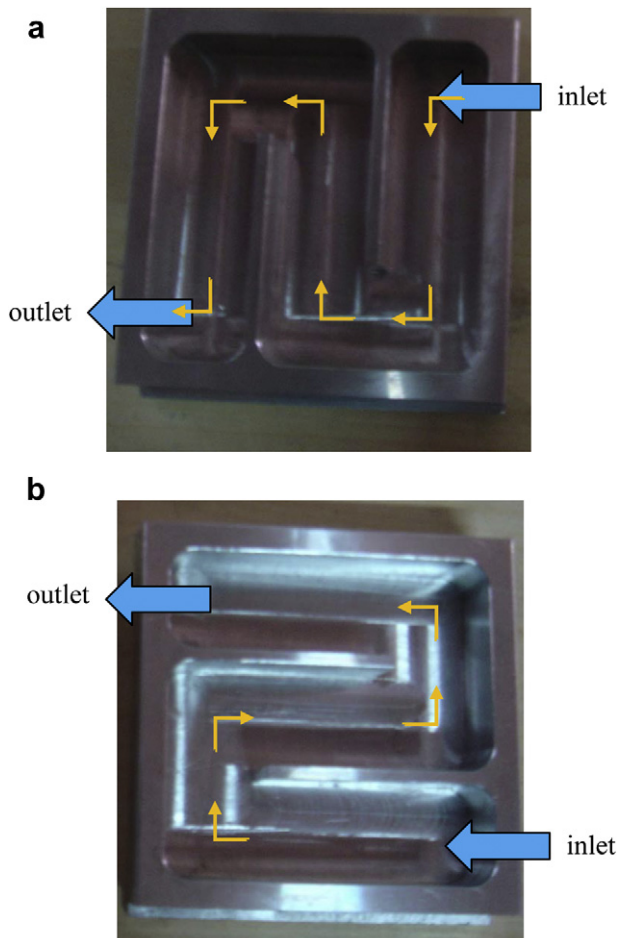


Fig. 2. The flow patterns of (a) Type A and (b) Type B heat sinks.

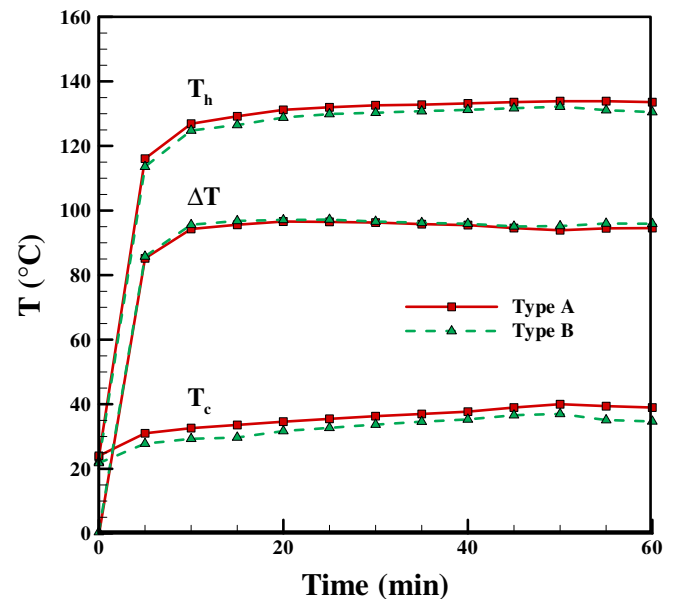


Fig. 3. Temporal temperature distributions of hot side (T_h), cold side (T_c) and their difference (ΔT) of the module with two types of heat sink.

flow pattern between Types A and B is that the flow direction of water and inlet is cross-current in the former whereas it is co-current in the latter, as shown in Fig. 2. As a result, the flow direction of water changes 6 times in Type A and 4 times in Type B. The temperature distributions at the hot side and the cold side as well as their difference with increasing time are shown in Fig. 3 where the heating temperature was 150 °C and the water flow rate was 1.0 L min⁻¹. It can be seen that the discrepancies in the curves between Types A and B are slight, that is, the temperature difference across the module under the two different heat sinks are similar. It is thus recognized that, with the aforementioned operating conditions, the effect of flow pattern in Types A and B on the TE module is not significant. Therefore, the two heat sinks are

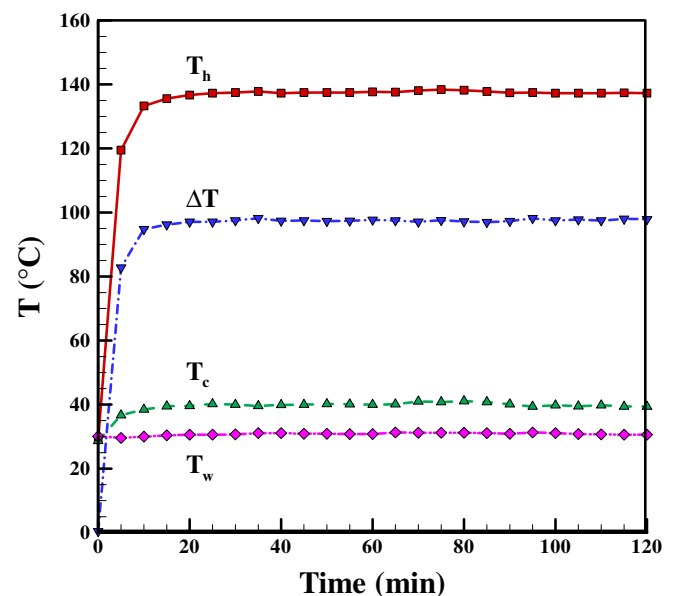


Fig. 4. Temporal temperatures distributions of hot side, cold side and their difference of the module and cooling water (T_w).

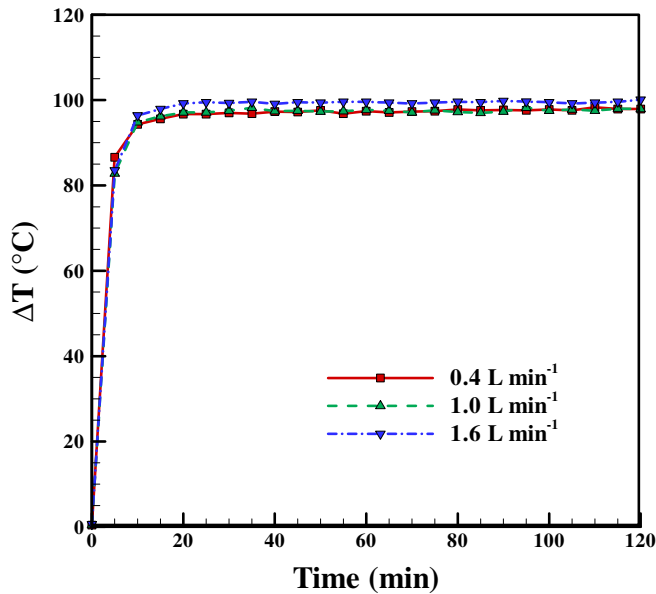


Fig. 5. Temporal distributions of temperature difference between the two sides of the module at various water flow rates with $T_H = 150$ °C.

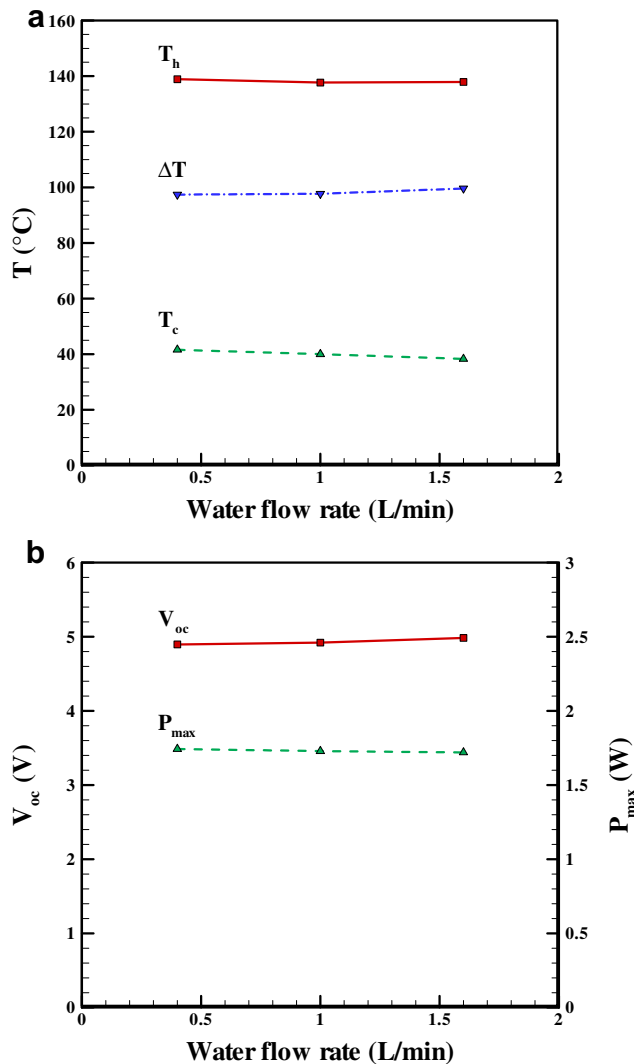


Fig. 6. Steady-state distributions of (a) temperature and (b) open circuit voltage and maximum output power at various water flow rates with $T_H = 150$ °C.

simultaneously used in the later experiments for TEMs in series to make the connection of water pipes conveniently. The following results concerning No. 1 TEM are obtained using Type A heat sink.

Furthermore, temporal distributions of temperatures of the cold side, hot side and water as well as the temperature difference between the two sides for No. 1 module at the conditions of 150 °C and 1.0 L min⁻¹ are demonstrated in Fig. 4. The temperatures at the two side rise rapidly in the initial period (≤ 10 min); afterward, their variations are slight. Alternatively, the temperature of water is kept at around 30 °C. This means that the combination of tank and axial fan can effectively transport heat from the cold side. Because the measured data at 60 min can represent the steady-state results, the following discussion is based on the data measured at 60 min.

3.2. Effect of flow rate of coolant

To realize the influence of flow rate of coolant on the performance of TEM, the temporal distributions of temperature difference of No. 1 TEM at the flow rates of 0.4, 1.0 and 1.6 L min⁻¹ are presented in Fig. 5 where the heating temperature was fixed at

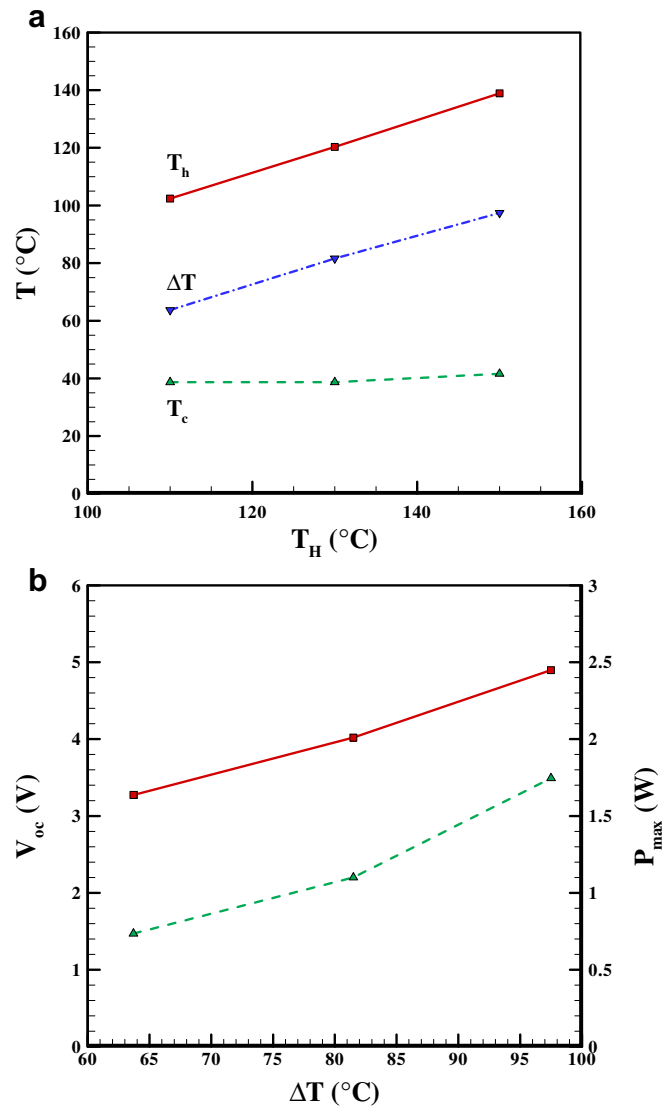


Fig. 7. Steady-state distributions of (a) temperature at various heating temperatures and (b) open circuit voltage and maximum output power versus temperature difference.

150 °C. It is apparent that the flow rate affecting the temperature difference across the module is slight. Similar behavior has been reported in the theoretical result of Esarte et al. [25]. Meanwhile, it is noted that the curves almost become horizontal when the experimental duration is as long as 60 min. Hence the data measured at 60 min can be considered as the steady-state results. Based on the measured data at the aforementioned moment, the profiles of steady-state temperatures at the hot and cold sides and their differences as well as open circuit voltage and the maximum output power at various flow rates are plotted in Fig. 6a and b. As shown in Fig. 6a, the temperatures at both the hot sides and the cold side merely decline a bit with increasing flow rate. Since the temperature drop at the cold side are larger than at the hot side when the flow rate goes up, this results in the slight increment in temperature difference. Specifically, the temperature differences corresponding to the flow rates of 0.4, 1.0 and 1.6 L min⁻¹ are 97.4, 97.7 and 99.6 °C, respectively. This also implies that the temperature difference is almost independent of water flow rate. As mentioned earlier, the thermoelectric conversion depends on the temperature difference across a module. Therefore, Fig. 6b depicts that the value of open circuit voltage somewhat increases from 4.90 to 4.98 V when the flow rate increases from 0.4 to 1.6 L min⁻¹, stemming from little increment in temperature difference. In regard to the maximum power, it is around 1.73 W where the electrical current is about 0.7 A. Because the performances of the module at the three flow rates are close to each other, and a larger flow rate means the larger power consumption of the pump, the low flow rate of 0.4 L min⁻¹ is adopted for further investigation below.

3.3. Effect of heating temperature

Subsequently, the influence of heating temperature on the performance of No. 1 TEM is examined in Fig. 7 where the flow rate of water was fixed at 0.4 L min⁻¹. It can be seen that the temperature of cold side is raised slightly when the heating temperature is lift from 110 to 150 °C, whereas the temperature of hot side is linearly proportional to the heating temperature (Fig. 7a). Consequently, the higher the heating temperature, the larger the temperature difference is. For the heating temperatures of 110, 130

and 150 °C, the temperature differences are 63.7, 81.6 and 97.4 °C, respectively. Corresponding to the preceding temperature differences, the open circuit voltage and the maximum power vary from 3.27 to 4.90 V and from 0.74 to 1.75 W, respectively (Fig. 7b). It is noteworthy that the increasing trend in the open circuit voltage and the maximum power is not linear, and a higher temperature difference amplifies the two physical scales. This characteristic is consistent with the studies of Champier et al. [10], Min and Rowe [24] and Gou et al. [29] and Hsu et al. [30]. Although the temperature difference, output voltage and power grow with heating temperature, the heating temperature is subject to the nature of TEM. The upper limit of heating temperature is restricted by the allowed maximum operating temperature of the TEMs. Consequently, the heating temperature is suggested at 150 °C which is the allowed maximum operating temperature of the tested modules in the study.

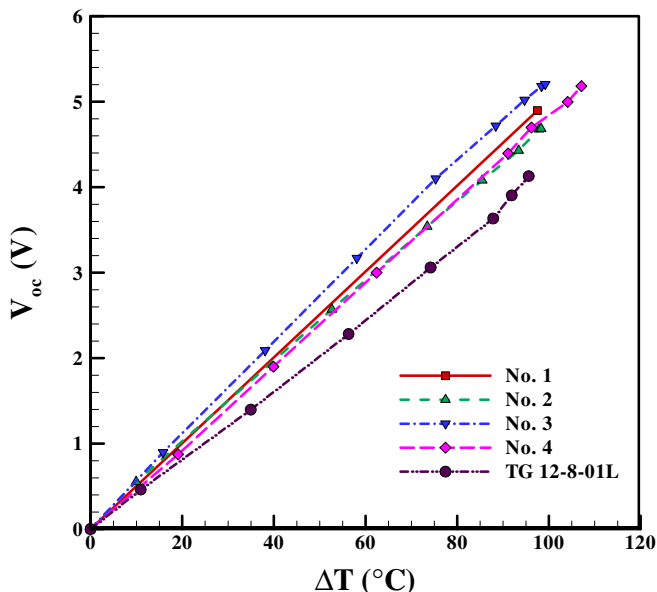


Fig. 8. Distributions of open circuit voltage of thermoelectric modules and generator.

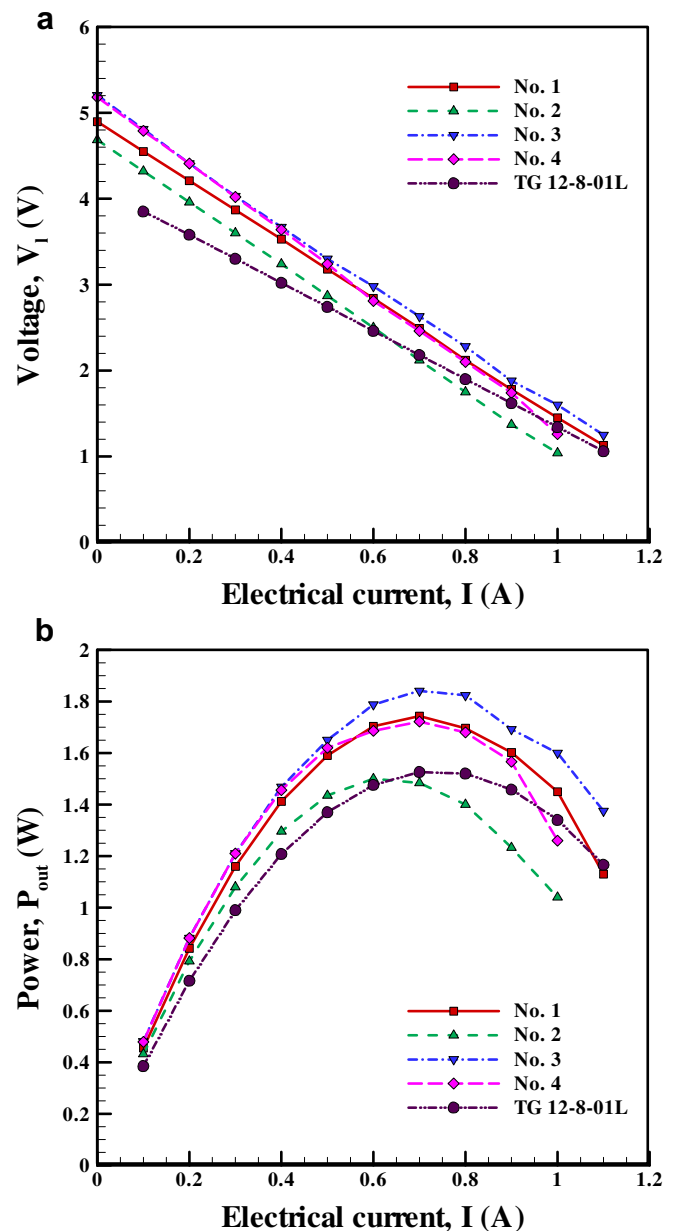


Fig. 9. Distributions of (a) output voltage and (b) power of thermoelectric modules and generator.

3.4. Comparison between TEM and TEG

The TEG is also tested at the same operating conditions to further examine the applicability of power generation from the TEM. The generator was provided by Marlow Industries; its type number is TG-12-8-01L (Table 2) and its size is close to the TEMs. With the heating temperature of 150 °C and water flow rate of 0.4 L min⁻¹, the temperature difference across the TEG is 95 °C which is close to the value of the tested TEM, 98 °C (Fig. 7). According to the preceding results, the slight discrepancy in the temperature differences can be neglected so that the baseline of the comparison is fixed. The profiles of open circuit voltage, output voltage and power of the four modules (i.e. Nos. 1–4) and the generator are shown in Figs. 8 and 9. It can be seen that the output performances of the TEMs are somewhat higher than that of the TEG under the same conditions. If one considers the costs of the TEM (7 USD per module) and the TEG (49 USD per generator), the TEMs would be more favorable for the applications of low-temperature waste-heat recovery. It is thus summarized that if the temperature of a system with waste heat is below 150 °C, TEM is the proper choice for power generation compared to that of TEG, from the cost point of view.

3.5. Performance of TEMs in series

Attention is then shifted to the performance of the TEMs in series with the heating temperature of 150 °C and water flow rate of 0.4 L min⁻¹ where the TEMs are connected from 1 to 4 (i.e. $N = 1$ –4). Moreover, both Types A and B heat sinks are linked alternatively to make the connection of water pipes more convenient. Fig. 10 indicates that the open circuit voltage and the maximum power are almost linearly proportional to the number of modules. This behavior has been reported in the theoretical study of Gou et al. [29]. For the four TEMs in series, the open circuit voltage and the maximum power are 19.48 V and 7.34 W, respectively, revealing that the more number of modules in series give the higher the maximum power. However, as shown in Fig. 11, there exists difference between the predictions and experimental measurements. The predictions are obtained in terms of the superposition of the individual performances of the TEMs. It can be seen that the predictions depart from the experimental data as the

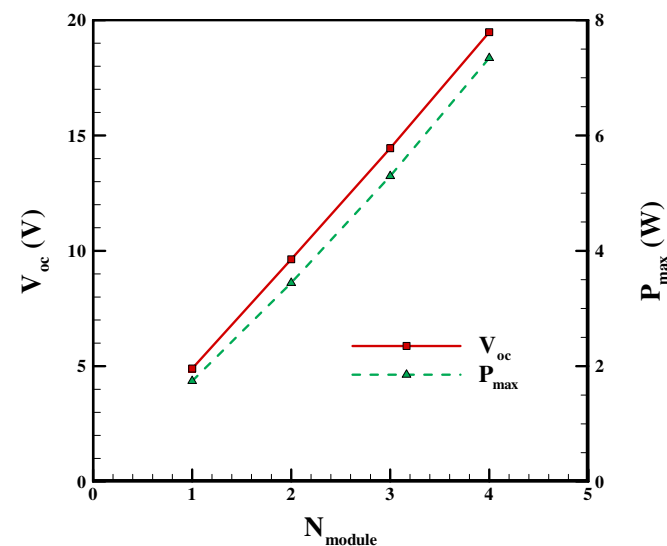


Fig. 10. Distributions of open circuit voltage and the maximum output power with number of modules in series.

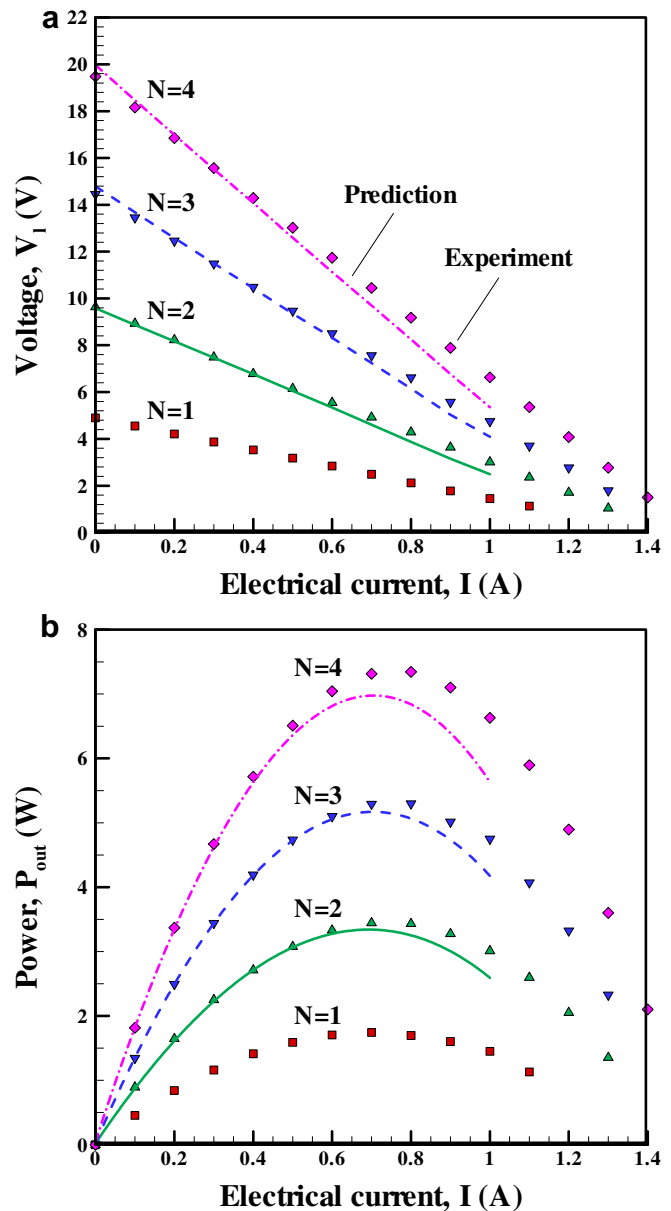


Fig. 11. Distributions of (a) output voltage and (b) power of thermoelectric modules in series versus electrical current.

electrical current increases, especially for the case of $N = 4$. It has been reported that, when the external load resistance becomes larger or the electrical current becomes smaller, the Peltier effect was less obvious which would cause an increase in temperature difference, output voltage and power [31]. Increasing N increases the external load resistance under the same electrical current. For example, corresponding to $N = 1, 2, 3$ and 4 , the values of external load resistance are 1.45, 3.01, 4.75 and 6.63 Ω , when the electrical current is fixed at 1.0 A. This is the reason that the output voltage and power from experimental data are larger than those of predictions.

Furthermore, the individual performances of the four modules are examined in the previous section. As shown in Fig. 8, the values of open circuit voltage of the four modules at the same temperature difference are different. Fig. 9a and b also reveal that the output voltage and power under the same electrical current are not identical when the temperature differences are around 98 °C. The

reason might be the non-uniform properties of the four modules due to the uncertainties in manufacturing process. Seeing that the thermoelectric properties of the four modules and the influence of the Peltier effect on the performance are not uniform, the linear relation may not be proper to be used in the series connection. In other words, the performance of thermoelectric modules in series cannot be simply predicted by adding the data of each module together, especially when the electrical current is large.

4. Conclusions

The characteristics of TEMs used for power generation by recovering low-temperature waste heat at different operating conditions have been investigated experimentally. The results show that the effect of flow pattern of Type A and B heat sinks on the performance of TEM is not apparent. With the condition of fixed heating temperature, the influence of water flow rate on the performance of the TEM is not obvious either. Consequently, in the current system, the lower water flow rate (0.4 L min^{-1}) is suggested for lower power consumption of pump. At a fixed water flow rate, increasing heating temperature leads to the better performance of the module. This reflects that power generation from the TEM depends strongly on the heat source. However, the temperature of heat source is subject to the allowed maximum operating temperature of TEM. Under appropriate operating conditions, the open circuit voltage, maximum power are linearly proportional to the number of modules in series ($N = 1\text{--}4$). Nevertheless, due to the Peltier effect and inherent non-uniformity among the TEMs, the performances of TEMs in series cannot be simply predicted by adding the data of each module together when electrical current is increased. The TEMs are suitable for power generation by recovering waste heat when the temperature of the system is lower than 150°C .

Acknowledgements

The authors acknowledge the financial support of the National Science Council, Taiwan, ROC, in this research.

References

- [1] Rowe DM. Thermoelectric handbook: macro to nano. 1st ed. Boca Raton, Florida, USA: CRC Press; 2006.
- [2] Gurevich YG, Logvinov GN. Physics of thermoelectric cooling. *Semicon Sci Technol* 2005;20:R57–64.
- [3] Simons RE, Ellsworth MJ, Chu RC. An assessment of module cooling enhancement with thermoelectric coolers. *ASME J Heat Transfer* 2005;127:76–84.
- [4] Wang CC, Hung CI, Chen WH. Design of heat sink for improving the performance of thermoelectric generator using a two-stage optimization. *Energy* 2012;39:236–45.
- [5] Wu KH, Hung CI. Thickness scaling characterization of thermoelectric module for small-scale electronic cooling. *J Chin Soc Mech Eng* 2009;30:475–81.
- [6] Chen WH, Liao CY, Hung CI. A numerical study on the performance of miniature thermoelectric cooler affected by Thomson Effect. *Appl Energy* 2012;89:464–73.
- [7] Martinez A, Astrain D, Rodriguez A. Experimental and analytical study on thermoelectric self cooling of devices. *Energy* 2011;36:5250–60.
- [8] Cheng TC, Cheng CH, Huang ZZ, Liao GC. Development of an energy-saving module via combination of solar cells and thermoelectric coolers for green building applications. *Energy* 2011;36:133–40.
- [9] Meng F, Chen L, Sun F. A numerical model and comparative investigation of a thermoelectric generator with multi-irreversibilities. *Energy* 2011;36:3513–22.
- [10] Champier D, Bedecarrats JP, Rivaletto M, Strub F. Thermoelectric power generation from biomass cook stoves. *Energy* 2010;35:935–42.
- [11] Champier D, Bedecarrats JP, Kousksou T, Rivaletto M, Strub F, Pignolet P. Study of a TE (thermoelectric) generator incorporated in a multifunction wood stove. *Energy* 2011;36:1518–26.
- [12] Thacher EF, Helenbrook BT, Karri MA, Richter CJ. Testing of an automobile exhaust thermoelectric generator in a light truck. *Proc Inst Mech Eng Part D J Automob Eng* 2007;221:95–107.
- [13] Thomas JP, Qidwai MA, Kellogg JC. Energy scavenging for small-scale unmanned systems. *J Power Sources* 2006;159:1494–509.
- [14] Riffat SB, Ma X. Thermoelectrics: a review of present and potential applications. *Appl Thermal Eng* 2003;23:913–35.
- [15] Zhang SJ, Wang HX, Guo T. Performance comparison and parametric optimization of subcritical organic Rankine cycle (ORC) and transcritical power cycle system for low-temperature geothermal power generation. *Appl Energy* 2011;88:2740–54.
- [16] Vélaz F, Segovia J, Chejne F, Antolín G, Quijano A, Martín MC. Low temperature heat source for power generation: exhaustive analysis of a carbon dioxide transcritical power cycle. *Energy* 2011;36:5497–507.
- [17] Boukai AI, Bunimovich Y, Tahir-Kheli J, Yu JK, Goddard III WA, Heath JR. Silicon nanowires as efficient thermoelectric materials. *Nature* 2008;451:168–71.
- [18] Poudel B. High-thermoelectric performance of nanostructured bismuth antimony telluride bulk alloys. *Science* 2008;320:634–8.
- [19] Bell LE. Cooling, heating, generating power, and recovering waste heat with thermoelectric systems. *Science* 2008;321:1457–61.
- [20] Chen WH, Chen JC. Combustion characteristics and energy recovery of a small mass burn incinerator. *Int Commun Heat Mass Transfer* 2001;28:299–310.
- [21] Chen WH, Chung YC, Liu JL. Analysis on energy consumption and performance of reheating furnaces in a hot strip mill. *Int Commun Heat Mass Transfer* 2005;32:695–706.
- [22] Hsiao YY, Cheng WC, Chen SL. A mathematic model of thermoelectric module with applications on waste heat recovery from automobile engine. *Energy* 2010;35:1447–54.
- [23] Anatyshuk LI, Luste OJ, Kuz RV. Theoretical and experimental study of thermoelectric generators for vehicles. *J Electron Mater* 2011;40:1326–31.
- [24] Min G, Rowe DM. Evaluation of thermoelectric modules for power generation. *J Power Sources* 1998;73:193–8.
- [25] Esarte J, Min G, Rowe DM. Modelling heat exchangers for thermoelectric generators. *J Power Sources* 2001;93:72–6.
- [26] Yu J, Zhao H. A numerical model for thermoelectric generator with the parallel plate heat exchanger. *J Power Sources* 2007;172:428–34.
- [27] Niu X, Yu J, Wang S. Experimental study on low-temperature waste heat thermoelectric generator. *J Power Sources* 2009;188:621–6.
- [28] Astrain D, Vian JG, Martinez A, Rodriguez A. Study of the influence of heat exchangers' thermal resistances on a thermoelectric generation system. *Energy* 2010;35:602–10.
- [29] Gou X, Xiao H, Yang S. Modeling, experimental study and optimization on low-temperature waste heat thermoelectric generator system. *Appl Energy* 2010;87:3131–6.
- [30] Hsu CT, Huang GY, Chu HS, Yu B, Yao DJ. Experiments and simulations on low-temperature waste heat harvesting system by thermoelectric power generators. *Appl Energy* 2011;88:1291–7.
- [31] Zhu J, Gao J, Chen M, Zhang J, Du Q, Rosendahl LA, et al. Experimental study of a thermoelectric generating system. *J Electron Mater* 2011;40:744–52.
- [32] Liang G, Zhou J, Huang X. Analytical model of parallel thermoelectric generator. *Appl Energy* 2011;88:5193–9.
- [33] Feeley TJ, Skone TJ, Stiegel GJ, McNemar A, Nemeth M, Schimmoller B, et al. Water: a critical resource in the thermoelectric power industry. *Energy* 2008;33:1–11.
- [34] Kline SJ. The purpose of uncertainty analysis. *ASME J Heat Transfer* 1985;107:153–60.
- [35] Coleman HW, Steele Jr WG. Experimentation and uncertainty analysis for engineers. New York: Wiley; 1989.